nature nanotechnology

SUPPLEMENTARY INFORMATION

https://doi.org/10.1038/s41565-019-0442-x

In the format provided by the authors and unedited.

Transition metal dichalcogenide nanodisks as high-index dielectric Mie nanoresonators

Ruggero Verre[1,2], Denis G. Baranov[1,2], Battulga Munkhbat[1], Jorge Cuadra[1], Mikael Käll[1]* and Timur Shegai[1]*

[1]Department of Physics, Chalmers University of Technology, Gothenburg, Sweden. [2]These authors contributed equally: Ruggero Verre, Denis G. Baranov.
*e-mail: mikael.kall@chalmers.se; timurs@chalmers.se

Supplementary Material for "Transition metal dichalcogenide nanodisks as high-index dielectric Mie nanoresonators".

Ruggero Verre,[+] *Denis G. Baranov,* [+] *Battulga Munkhbat, Jorge Cuadra, Mikael Käll,* Timur Shegai**

Department of Physics, Chalmers University of Technology, 412 96 Göteborg, Sweden

*email: mikael.kall@chalmers.se; timurs@chalmers.se

Table of Context:

1. CONFOCAL RAMAN ANALYSIS

2. OPTICAL CHARACTERIZATION AND ANAPOLE ANALYSIS IN WS_2 NANODISKS

3. HAMILTONIAN MODEL OF ANAPOLE-EXCITON COUPLING

1. CONFOCAL RAMAN ANALYSIS

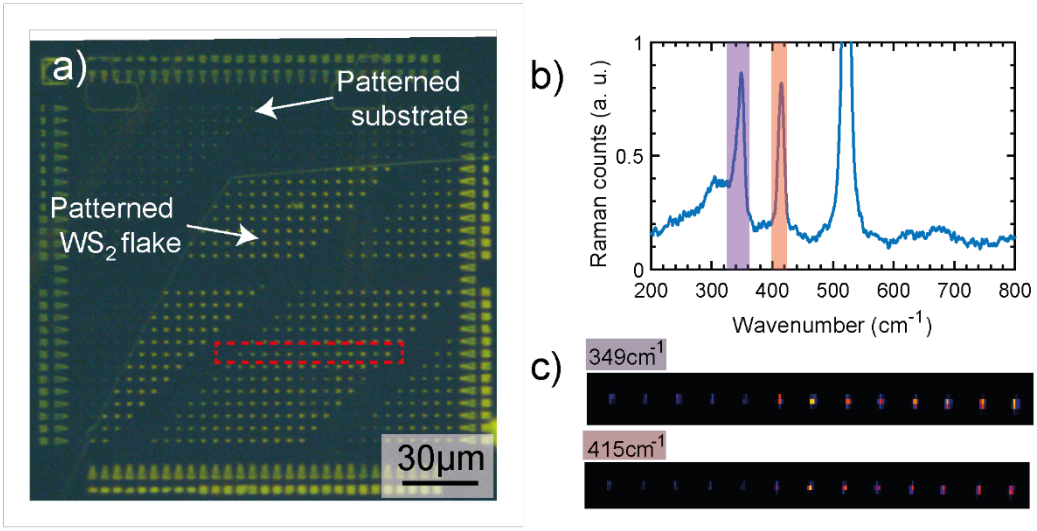

Figure S1. (a) Dark field image of the edge of a WS_2 flake after nanopatterning, demonstrating significant optical contrast between the patterned nanodisks and the substrate. Nanodisks with different sizes were patterned. (b) Each nanoparticle is composed of single crystalline WS_2 as confirmed by the Raman lines at 349 cm^{-1} and 415 cm^{-1} (the intense phonon line at ~522 cm^{-1} originates from the Si substrate underneath). (c) Wavenumber-specific confocal Raman maps obtained from the area indicated by the red rectangle in panel (a). The measurements confirm complete removal of WS_2 in the etched region around each nanodisk.

2. OPTICAL CHARACTERIZATION, SIMULATIONS AND ANAPOLE ANALYSIS IN WS_2 NANODISKS

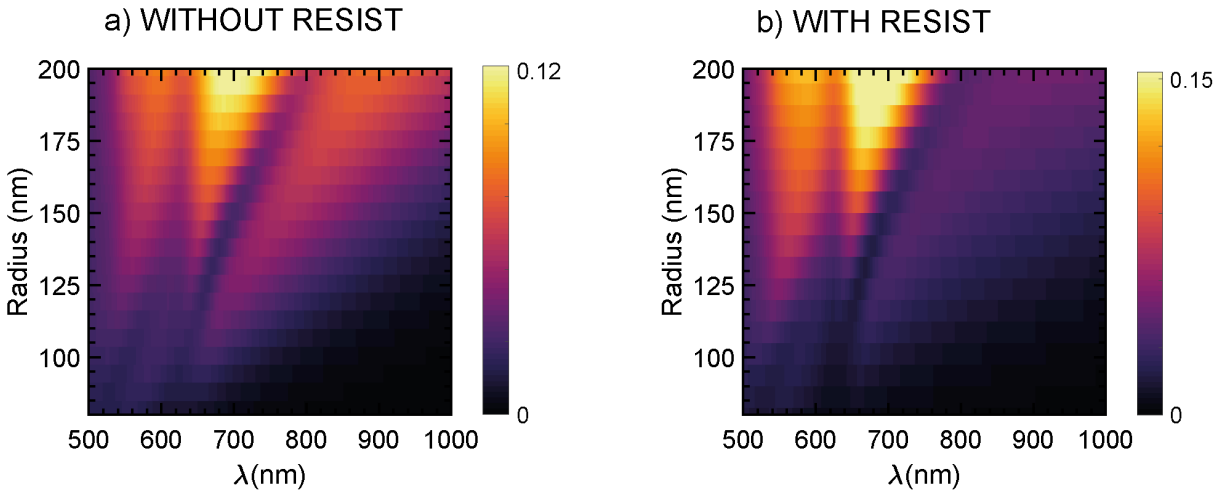

Figure S2. Simulated backward scattering cross-section in μm^2 for a WS_2 nanodisk on a SiO_2(55 nm)/Si substrate as a function of radius and with a height of 55 nm. The difference is the presence of a transparent (n=1.5) nanodisk with a height of 300 nm on top of the WS_2 disk.

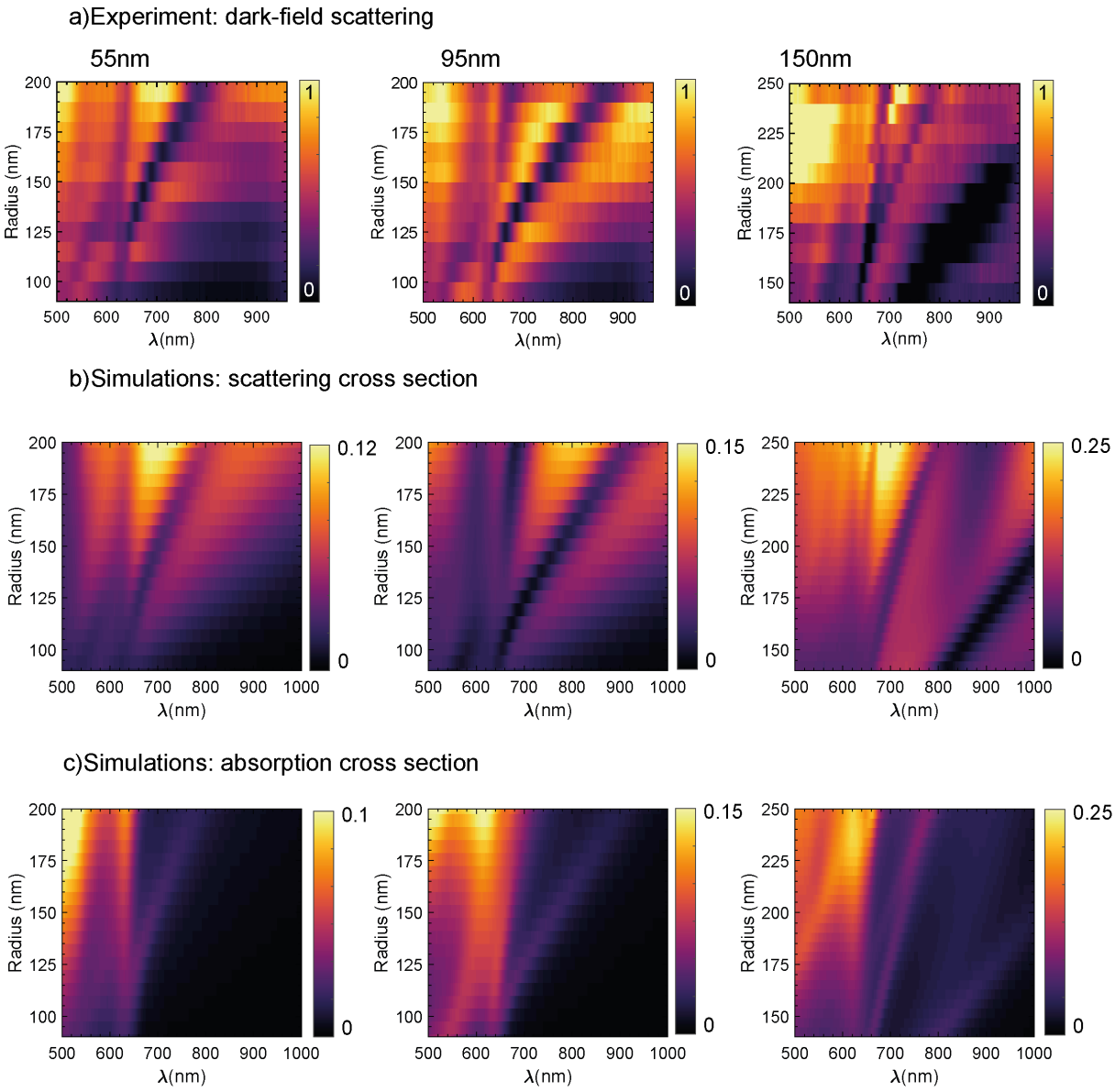

Figure S3. (a) Experimental dark-field scattering spectra of WS_2 nanodisks, placed on a SiO_2(55 nm)/Si substrate, as a function of the radius for the heights of 55 nm, 95 nm, and 150 nm. Simulated back-scattering (b) and absorption (c) cross-sections in μm^2.

In the experiments conducted in this study, side illumination was used, and the scattering collected with a low NA objective (see methods). Nanodisks on a substrate were simulated using a TFSF source at normal incidence and the scattering was analyzed in the full backward direction using a transmission monitor. For reciprocity arguments, this is a reasonable approximation and it can qualitatively reproduce the experimental observation.

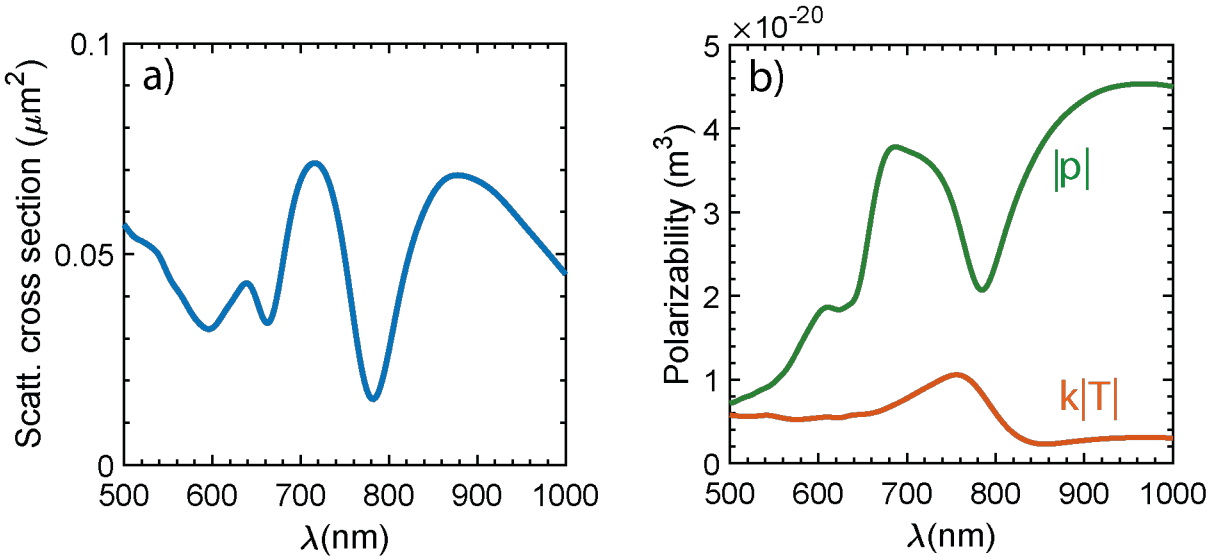

Figure S4. (a) Simulated scattering cross-section for a nanodisk of 95 nm height and 150 nm radius. An anapole dip is found at ~780nm. (b) Cartesian multipole decomposition of induced polarization in the same nanodisk. Although the two curves do not cross in correspondence of the anapole dip, they pull towards each other and it correlates with the scattering dip. The ideal anapole state does not arise in this system due to dissipative losses, which do not allow total suppression of scattering according to the optical theorem. Nevertheless, far-field scattering shows a clear scattering dip and the simulated spatial distribution of the electric field inside the disk exhibits the distinct anapole-like pattern, Fig. 2, corroborating the anapole nature of the scattering dip.

3. HAMILTONIAN MODEL OF ANAPOLE-EXCITON COUPLING

S3.1 DIELECTRIC FUNCTION AND RADIUS DEPENDENCE OF THE ARTIFICIAL MATERIAL

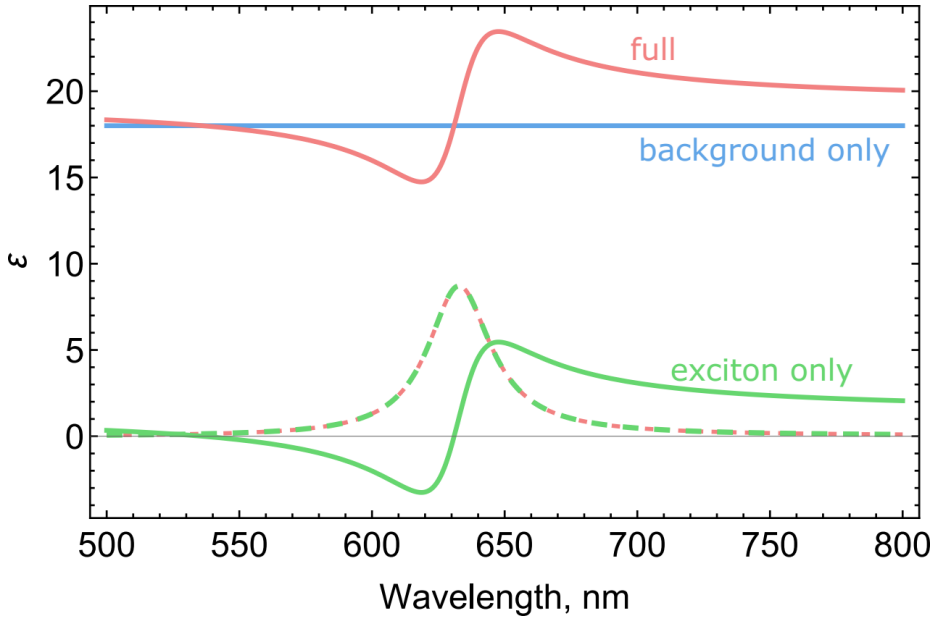

Figure S5. Artificial permittivities used to simulate scattering from nanodisks made of a hypothetical exciton-only nanodisk (green lines), lossless high-index nanodisk (blue line), and sum of these permittivities (red lines). Solid lines show real parts, dashed lines show imaginary parts.

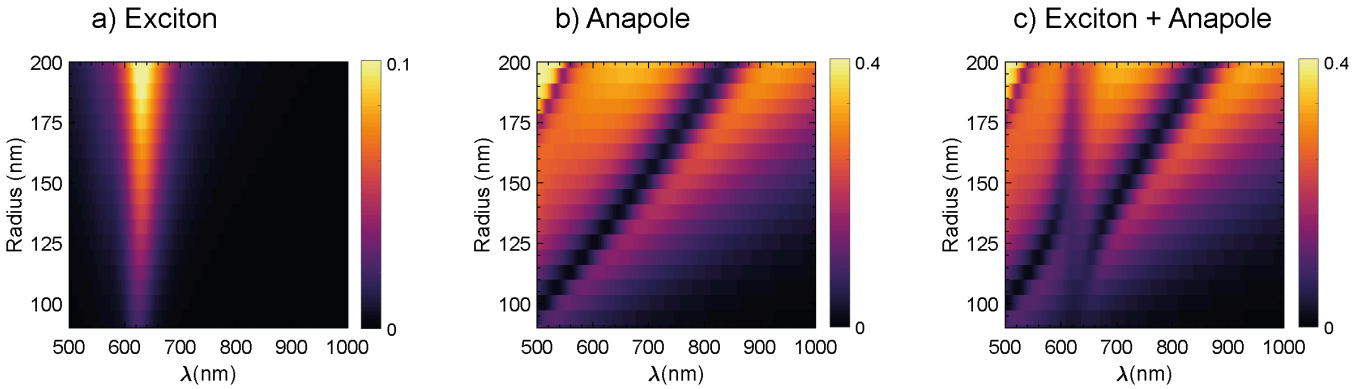

Figure S6. Simulated FDTD scattering cross-section map in μm^2 for nanodisks of 55 nm height in air obtained using different artificial permittivities shown in Fig. S5. (a) exciton-only nanodisk, (b) lossless high-index nanodisk, and (c) the total permittivity accounting for both.

S3.2 HAMILTONIAN FORMALISM

To interpret the experimental results, we use a Hamiltonian model built on the basis of the temporal coupled mode theory [1,2]. It incorporates three coupled modes (oscillators): a "broad" Mie mode of the nanodisk ('b'), providing a broad and intense scattering background in the response, a narrow "dark" Mie mode ('d'), and a non-radiative exciton transition ('X'). The system's response is described by a ket-vector of complex amplitudes $|a\rangle = (a_b, a_d, a_X)^T$. The dynamics of the amplitudes is governed by the Schrödinger-like equation [1,2]:

$$i\frac{d|a\rangle}{dt} = \widehat{H}|a\rangle + |\kappa\rangle s_+, \tag{S1}$$

where $\widehat{H}$ is the Hamiltonian of the coupled system, s_+ is the scalar amplitude of the incident wave, and $|\kappa\rangle = \left(\sqrt{\gamma_b^{rad}/2}, \sqrt{\gamma_d^{rad}/2}, 0\right)^T$ is the ket-vector of radiative coupling constants.

Under a harmonic excitation $s_+(t) = s_+ e^{-i\omega_0 t}$ the mode amplitudes oscillate at the driving frequency, $|a(t)\rangle \propto e^{-i\omega_0 t}$. The steady state solution therefore can be formally written as

$$|a\rangle = s_+\left[i(\widehat{H} - \hat{I}\omega_0)\right]^{-1}|\kappa\rangle, \tag{S2}$$

where $\hat{I}$ is the unity operator and $\left[i(\widehat{H} - \hat{I}\omega_0)\right]^{-1}$ is the resolvent of $\widehat{H}$. The structure of this solution highlights two essential contributions to the steady state amplitudes: $|\kappa\rangle$ shows the strength of the oscillators coupling to the incident radiation field, whereas the resolvent encodes all information about positions of the resonances of the system.

The Hamiltonian describing the system has the following form:

$$\widehat{H} = \hbar\begin{bmatrix} \omega_b - i\gamma_b/2 & -i\sqrt{\gamma_b^{rad}\gamma_d^{rad}/4} & g_{bX} \\ -i\sqrt{\gamma_b^{rad}\gamma_d^{rad}/4} & \omega_d - i\gamma_d/2 & g_{dX} \\ g_{bX} & g_{dX} & \omega_X - i\gamma_X/2 \end{bmatrix}, \tag{S3}$$

where ω_b and ω_d are the frequencies of the two geometric modes, ω_X is the exciton frequency, γ_b, γ_d, and γ_X are the linewidths of the respective resonances. The off-diagonal element g_{bX} and g_{dX} reflects the near-field coupling between the broad and the dark Mie

modes and the exciton, respectively, whereas the anti-Hermitian term $-i\sqrt{\gamma_b^{rad}\gamma_d^{rad}}/4$ reflects the far-field interference between the two Mie modes [3].

Intensity of the scattered signal reads

$$\text{Scat} = |s_-|^2 = |Cs_+ + \langle a|\kappa\rangle|^2, \tag{S4}$$

where C is the direct scattering matrix that can be assumed to be 0 for an isolated nanoparticle and plane wave illumination. Correspondingly, the absorption is given by

$$\text{Abs} = \gamma_b^{non-rad}|a_b|^2 + \gamma_d^{non-rad}|a_d|^2 + \gamma_X|a_X|^2. \tag{S5}$$

Transient dynamics of the populations upon initial excitation of the exciton was calculated using the Schrödinger-like equation (S1) in the absence of the driving field s_+. The population of each mode was then found as the squared absolute value of the oscillator's amplitudes $|a_i(t)|^2$.

S3.3. EXTRACTION OF THE PARAMETERS FOR STRONG COUPLING ANALYSIS

We extracted the parameters of the Hamiltonian (S3) by fitting the scattering and absorption spectra numerically calculated with FDTD for a nanodisk using the different dielectric functions plotted in Fig. S5. The procedure involves several steps:

1) **Determination of the narrow geometric mode eigen energies for a large permittivity nanodisk.** For simplicity, in our formalism we assume at first a dispersionless material with permittivity $\varepsilon = 18 + 0.01i$. We performed FDTD simulation for nanodisks with a fixed height of 55 nm as a function of the radius. We first fitted the *absorption* spectrum (Fig. S7a) and extracted the eigenfrequency ω_d and the total (sum of radiative and non-radiative) linewidth $\gamma_d = \gamma_d^{rad} + \gamma_d^{non-rad}$ of the dark mode. During the fitting, we only imposed a linear dispersion of the resonant wavelength of the mode with the disk radius.
2) **Determination of the broad geometric mode eigen energies for a large permittivity nanodisk.** In order to determine ω_b, γ_b^{rad} and the relative ratio between γ_d^{rad} and $\gamma_d^{non-rad}$, we fitted the *scattering* spectra of the same nanodisks (Fig. S7b). It is interesting to note that the absorption peak for the disk is closely related to the

anapole dip observed in scattering. To reproduce the anapole dip, we considered interference between the broad and narrow modes by using the same formalism described in section 3.2 for the 2×2 Hamiltonian. During the fitting, we also assumed a linear dispersion of the broad mode resonant wavelength with the disk radius. The fitted parameters were uniquely determined using the total scattering amplitude as a single free parameter. The scattering calculated using the fitted values and the equation (S4) qualitatively well reproduces the one obtained by FDTD (Fig. S7c).

3) **Determination of the coupling constants.** For the 3×3 Hamiltonian, we used the values extracted in steps 1-2. The only incognita in the Hamiltonian are thus the coupling constants between the exciton and the two geometrical modes. We calculated using FDTD the scattering spectra from a nanodisk as a function of radius using a permittivity composed by the sum of the large background permittivity and the exciton. The scattering spectra, shown in Fig. 3d of the main text, are then fitted by radius-independent coupling constants g_{bX} and g_{dX} with the 3×3 Hamiltonian model described in section S3.2. The fitted parameters, radiative and non-radiative components and coupling constants are shown in Fig. S8 as a function of the nanodisk radius. The scattering spectrum in Fig. 3f was obtained by applying equation (S4) to the full 3×3 Hamiltonian.

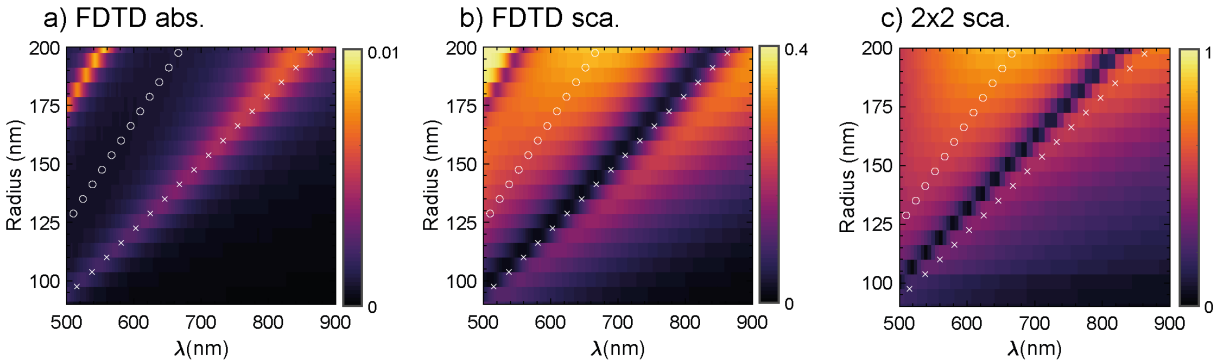

Figure S7. Maps of FDTD simulated (a) absorption and (b) scattering cross-section map in μm^2 by 55 nm height nanodisks in air obtained using the artificial permittivity of $\varepsilon = 18 + 0.01i$. (c) Normalized scattering map calculated with the 2×2 Hamiltonian model using the fitted values.

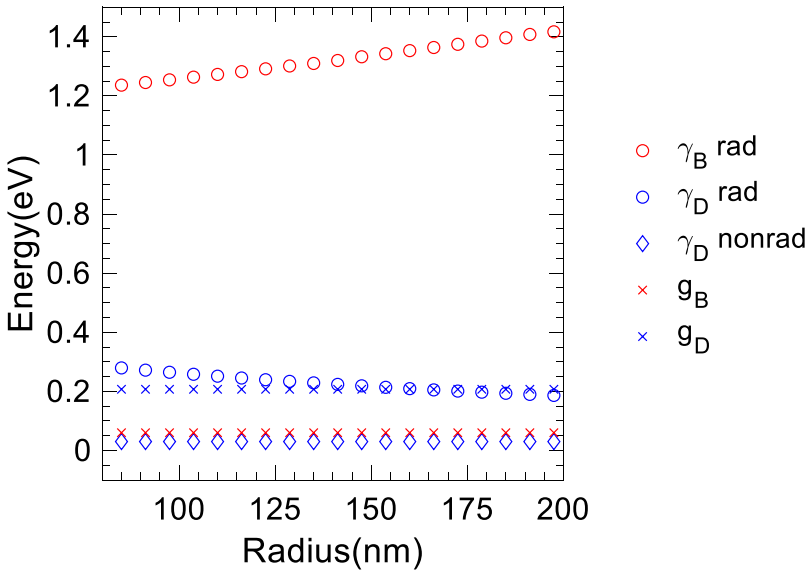

Figure S8. Radius-dependent parameters obtained by the fitting procedure described in section S3.3. Note that $\gamma_b^{non-rad}$ was assumed to be 0 and it is thus not plotted.

Supplementary References:

[1] H. Haus, Waves and Fields in Optoelectronics (Prentice Hall, Englewood Cliffs, NJ, 1984).

[2] S. Fan, W. Suh, and J. D. Joannopoulos, J. Opt. Soc. Am. B 20, 569 (2003).

[3] W. Suh, Z. Wang, and S. Fan, IEEE J. Quantum Electron. 40, 1511–1518 (2004).

[4] Y. Li et al., Phys. Rev. B **90**, 205422, (2014).